Monsoons in a changing world: A regional perspective in a global context

Akio Kitoh,[1] Hirokazu Endo,[1] K. Krishna Kumar,[2] Iracema F. A. Cavalcanti,[3] Prashant Goswami,[4] and Tianjun Zhou[5]

Received 15 September 2012; revised 8 February 2013; accepted 11 February 2013; published 19 April 2013.

[1] We provide a new view of global and regional monsoonal rainfall, and their changes in the 21st century under RCP4.5 and RCP8.5 scenarios as projected by 29 climate models that participated in the Coupled Model Intercomparison Project phase 5. The model results show that the global monsoon area defined by the annual range in precipitation is projected to expand mainly over the central to eastern tropical Pacific, the southern Indian Ocean, and eastern Asia. The global monsoon precipitation intensity and the global monsoon total precipitation are also projected to increase. Indices of heavy precipitation are projected to increase much more than those for mean precipitation. Over the Asian monsoon domain, projected changes in extreme precipitation indices are larger than over other monsoon domains, indicating the strong sensitivity of Asian monsoon to global warming. Over the American and African monsoon regions, projected future changes in mean precipitation are rather modest, but those in precipitation extremes are large. Models project that monsoon retreat dates will delay, while onset dates will either advance or show no change, resulting in lengthening of the monsoon season. However, models' limited ability to reproduce the present monsoon climate and the large scatter among the model projections limit the confidence in the results. The projected increase of the global monsoon precipitation can be attributed to an increase of moisture convergence due to increased surface evaporation and water vapor in the air column although offset to a certain extent by the weakening of the monsoon circulation.

Citation: Kitoh, A., H. Endo, K. Krishna Kumar, I. F. A. Cavalcanti, P. Goswami, and T. Zhou (2013), Monsoons in a changing world: A regional perspective in a global context, *J. Geophys. Res. Atmos.*, *118*, 3053–3065, doi:10.1002/jgrd.50258.

1. Introduction

[2] The monsoon is conventionally defined as a seasonal reversal of prevailing surface winds, driven by the seasonal cycle of solar heating and difference in thermal inertias of land and ocean that establish a land-sea temperature difference [*Webster and coauthors*, 1998]. This large-scale wind reversal creates favorable conditions for the occurrence of convection in the summer hemisphere. As the monsoon season matures, latent heat released by convection high above the land surface helps to draw additional moisture over the land from nearby oceans, maintaining the wet season. Monsoons are responsible for the majority of summer rainfall within the tropics, where billions of people depend on the monsoon-related rainfall. Patterns of projected global-scale changes in the surface temperatures are robust among models, with greater warming over land than over ocean and at most high latitudes [*Meehl and coauthors*, 2007]. Therefore, the land-sea temperature contrast is projected to become larger in summer, together with ample moisture available in a warming world, leading to a more intense monsoon. However, in spite of their common basic mechanism, monsoons over different regions are subject to diverse forcing; thus the responses of the various regional monsoons to a changing climate are expected to vary [*Meehl et al.*, 2007; *Turner and Annamalai*, 2012].

[3] The monsoon region is distributed over all the tropical continents, and over the tropical oceans in the western North Pacific, eastern North Pacific, and the southern Indian Ocean [*Wang and Ding*, 2006]. Although the American monsoons are not characterized by a seasonal reversal of wind, there are large differences in precipitation, humidity, and atmospheric circulation between summer and winter [*Vera and coauthors*, 2006; *Raia and Cavalcanti*, 2008; *Marengo and coauthors*, 2010]. While different indices have been used to identify the lifecycle of monsoons, the definition of the monsoon in terms of the precipitation characteristics [*Wang and LinHo*, 2002; *Wang and Ding*, 2006] rather than

[1]Meteorological Research Institute, Tsukuba, Ibaraki, Japan.
[2]Indian Institute of Tropical Meteorology, Pune, India.
[3]Center for Weather Forecasting and Climate Studies (CPTEC), National Institute for Space Research (INPE), Cachoeira Paulista, SP, Brazil.
[4]CSIR Centre for Mathematical Modelling and Computer Simulations (C-MMACS), Bangalore, India.
[5]LASG, Institute of Atmospheric Physics, Chinese Academy of Sciences, Beijing, China.

Corresponding author: A. Kitoh, Climate Research Department, Meteorological Research Institute, 1-1 Nagamine, Tsukuba, Ibaraki 305-0052, Japan. (kitoh@mri-jma.go.jp)

2169-897X/13/10.1002/jgrd.50258

the wind reversal, permits the use of similar monsoon indices for all the monsoon regions (keeping in mind that rainfall is the lifeline for billions of people living there). Thus, from a global point of view, precipitation characteristics over South Asia, East Asia, Australia, Africa, and the Americas can be viewed as an integrated global monsoon system, associated with a global-scale persistent atmospheric overturning circulation [*Trenberth et al*., 2000]. *Wang and Ding* [2008] have demonstrated that the global monsoon is the dominant mode of the annual variation of the tropical circulation, characterizing the seasonality of the tropical climate.

[4] Examination of historical precipitation records over the monsoon regions around the globe reveals a decreasing trend in the global *land* monsoon precipitation over the last half of the 20th century (1948–2003), with primary contributions from a weakening of the summer monsoon systems in the Northern Hemisphere (NH) [*Wang and Ding*, 2006; *Ramesh and Goswami*, 2007; *Zhou et al*., 2008b]. Changes in both the monsoon area and monsoon intensity contribute to this decreasing tendency [*Zhou et al*., 2008a]. However, the combined (oceanic and land) monsoon precipitation has increased for the more recent 1979–2008 epoch mainly due to a significant upward trend in the NH summer monsoon precipitation [*Wang et al*., 2012]. When the change in monsoon-affected domain is considered, the fractional increase in monsoon area is greater than in total precipitation, so that the ratio of these two measures (which serves as an index of the global monsoon intensity) exhibits a decreasing trend for the most recent 30 year (1979–2008) period [*Hsu et al*., 2011].

[5] *Kim et al*. [2008] investigated the reproducibility of global monsoon climate variability simulated by the coupled global climate models (CGCM) that participated in the Coupled Model Intercomparison Project phase 3 (CMIP3). They found that the CMIP3 CGCM multimodel ensemble simulates a reasonably realistic climatology of the global monsoon precipitation and circulation, but models have common biases such as a northeastward shift of the Intertropical Convergence Zone (ITCZ) over the tropical North Pacific. *Kim et al*. [2008] also pointed out that models with higher resolution generally reproduced a better spatial pattern of the global monsoon precipitation compared to lower-resolution models. *Hsu et al*. [2012] investigated global monsoon area and precipitation in the late 21st century using three high-resolution atmospheric GCMs (40 km MPI ECHAM5, 20 km MRI/JMA, and 50 km GFDL HiRAM) that were forced by different future sea surface temperature (SST) warming patterns. They found a consistent increase in the global monsoon area, precipitation, and intensity among the model projections.

[6] Recently, many climate modeling groups around the world have participated in the Coupled Model Intercomparison Project phase 5 (CMIP5), under which a series of experiments including the 20th century historical simulation and 21st century climate projections with four different representative concentration pathway (RCP) scenarios were performed [*Taylor et al*., 2012]. There is evidence that the CMIP5 models are better than the CMIP3 models in simulating the Asian-Australian monsoon system. Several works [*Li et al*., 2012; *Sperber et al*., 2012] have reported that the CMIP5 multimodel mean is more skillful than the CMIP3 multimodel mean; however, the CMIP5 models' simulation of El Niño-Southern Oscillation-monsoon relationships is still found to be poor (correlation is too weak). *Lee and Wang* [2012] and *Hsu et al*. [2013] found an increase of global monsoon area and precipitation intensity under the RCP4.5 scenario in CMIP5 model simulations of future changes in the global monsoon. These results are essentially consistent with CMIP3 model results [*Hsu et al*., 2012, 2013] but with some regional differences [*Lee and Wang*, 2012]. The objective of this paper is to provide an updated view of global and regional monsoonal rainfall and changes in the 21st century as projected by 29 CMIP5 models under the RCP4.5 and RCP8.5 scenarios: our analysis includes not only mean precipitation but also some precipitation extreme indices and monsoon seasonality changes for seven land monsoon regions across the world.

2. Data

2.1. Global Climate Model Data

[7] Table 1 lists the models used in our analysis. We used monthly mean data from 29 CMIP5 models and daily precipitation data from 21 CMIP5 models. Results from historical (1986–2005), RCP4.5 (2080–2099), and RCP8.5 (2080–2099) experiments were investigated. Only one ensemble member from each model was used. The grid squares where the land fraction exceeds 10% were regarded as land area in the analysis. Further information on the experiments and the models is available from the CMIP5 web site (http://cmip-pcmdi.llnl.gov/cmip5/).

2.2. Observed Precipitation Data for Validation

[8] We used Climate Prediction Center Merged Analysis of Precipitation (CMAP) [*Xie and Arkin*, 1997], Global Precipitation Climatology Project (GPCP) [*Huffman et al*., 2009], Climatic Research Unit Time-Series 3.1 (updated from *Mitchell and Jones* [2005]), Global Precipitation Climatology Centre Full Reanalysis version 6 (GPCC v.6) (updated from *Rudolf et al*. [1994]), Variability Analysis of Surface Climate Observations (GPCC-VASClimO) [*Beck et al*., 2005], GPGP One-Degree Daily data (GPCP 1DD) Version 1.2 [*Huffman et al*., 2001], and Tropical Rainfall Measuring Mission (TRMM) 3B42 product in version 6 [*Huffman et al*., 2007]. Note that GPCC-VASClimO is gridded data (0.5 degrees × 0.5 degrees) designed for climate variability and trend studies, based on time series of 9343 stations covering at least 90% of the period 1951–2000. All the observational data were first regridded onto a common 2.5 degree × 2.5 degree resolution (but GPCP 1DD and TRMM 3B42 were regridded onto 2.0 degree × 2.0 degree resolution).

2.3. Definition of Monsoon Domains, Onset, Retreat, and Duration

[9] A monsoon domain is defined where the annual range of precipitation exceeds 2.5 mm d^{-1}, based on the definition of *Wang et al*. [2011]. Here the annual range is defined as the difference between the May-September (MJJAS) mean and the November-March (NDJFM) mean. Monsoon onset date, retreat date, and its duration are determined using the criteria proposed by *Wang and LinHo* [2002] utilizing only precipitation data. Based on the regionally averaged relative climatological mean daily precipitation, which is the difference

Table 1. List of CMIP5 Models Used in This Study

Model ID	Institute ID	Country	Horizontal (Lon. × Lat.)		Monthly	Daily
ACCESS1-0	CAWCR	Australia	192×145	1.875×1.25	✓	✓
ACCESS1-3	CAWCR	Australia	192×145	1.875×1.25	✓	
bcc-csm1-1	BCC	China	128×64	T42	✓	✓
CanESM2	CCCMA	Canada	128×64	T63 (TL63)	✓	✓
CCSM4	NCAR	USA	288×192	1.25×0.942	✓	✓
CESM1-BGC	NCAR	USA	288×192	1.25×0.942	✓	✓
CESM1-CAM5	NCAR	USA	288×192	1.25×0.942	✓	
CNRM-CM5	CNRM/CERFACS	France	256×128	TL127	✓	✓
CSIRO-Mk3-6-0	CSIRO/QCCCE	Australia	192×96	T63	✓	✓
FGOALS-g2	LASG/IAP	China	128×60	2.8×3.1	✓	
FGOALS-s2	LASG/IAP	China	128×108	R42	✓	✓
GFDL-CM3	GFDL	USA	144×90	2.5×2	✓	
GFDL-ESM2G	GFDL	USA	144×90	2.5×2	✓	✓
GFDL-ESM2M	GFDL	USA	144×90	2.5×2	✓	✓
GISS-E2-R	GISS	USA	144×90	2.5×2	✓	
HadGEM2-CC	MOHC	UK	192×145	1.875×1.25	✓	
HadGEM2-ES	MOHC	UK	192×145	1.875×1.25	✓	
INM-CM4	INM	Russia	180×120	2×1.5	✓	✓
IPSL-CM5A-LR	IPSL	France	96×96	3.75×1.895	✓	✓
IPSL-CM5A-MR	IPSL	France	144×143	2.5×1.268	✓	✓
IPSL-CM5B-LR	IPSL	France	96×96	3.75×1.895	✓	✓
MIROC-ESM	MIROC	Japan	128×64	T42	✓	✓
MIROC-ESM-CHEM	MIROC	Japan	128×64	T42	✓	✓
MIROC5	MIROC	Japan	256×128	T85	✓	✓
MPI-ESM-LR	MPI-M	Germany	192×96	T63	✓	✓
MPI-ESM-MR	MPI-M	Germany	192×96	T63	✓	✓
MRI-CGCM3	MRI	Japan	320×160	TL159	✓	✓
NorESM1-M	NCC	Norway	144×96	2.5×1.895	✓	✓
NorESM1-ME	NCC	Norway	144×96	2.5×1.895	✓	

between the climatological daily precipitation and dry month (January in NH and July in the Southern Hemisphere (SH)) mean precipitation, the onset (retreat) date is defined as the date when the relative precipitation first exceeds (last drops below) 5 mm d^{-1}, and the duration is defined as their difference. The daily climatology of precipitation was defined as the sum of the first 12 harmonics of daily average precipitation.

2.4. Extreme Precipitation Indices

[10] We used four precipitation indices: average precipitation (Pav), simple precipitation daily intensity index (SDII), seasonal maximum 5 day precipitation total (R5d), and seasonal maximum consecutive dry days (CDD). Here SDII is defined as the total precipitation divided by the number of days with precipitation greater than or equal to 1 mm. R5d is defined as the seasonal maximum precipitation total in five consecutive days. CDD is defined as the seasonal maximum number of consecutive dry days with precipitation less than 1 mm. These indices were calculated for the summer season (MJJAS in NH and NDJFM in SH). All the extreme precipitation indices for the models were at first calculated for their original grid, and then averaged over each monsoon domain.

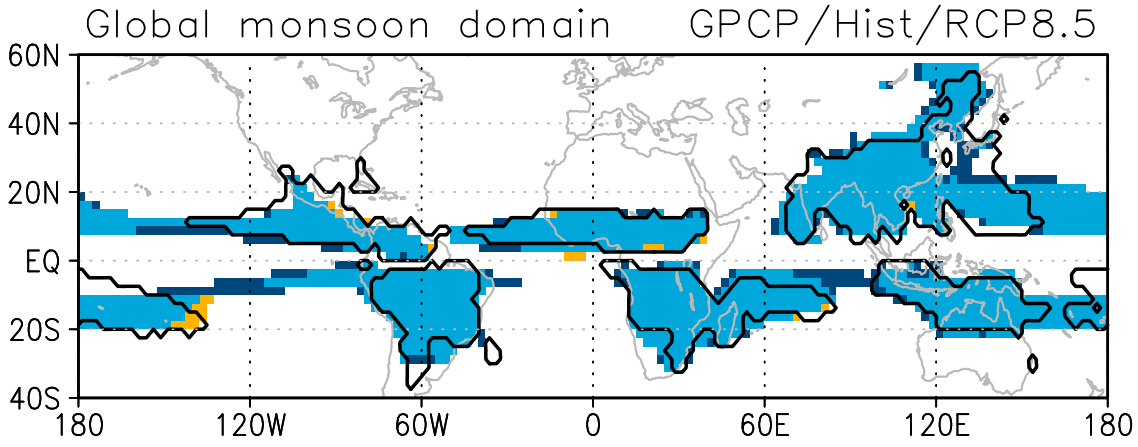

Figure 1. Observed (thick contour) and simulated (shading) global monsoon domain, based on the definition by *Wang et al.* [2011]. The observation is based on GPCP data, and the simulations are based on 29 CMIP5 multimodel mean precipitation with a common 2.5 by 2.5 degree grid in the present-day (1986–2005) and the future (2080–2099; RCP8.5 scenario). Warm yellow (dark blue) shading: monsoon domain only in the present-day (future). Blue shading: monsoon domain in the both periods.

3. Global Monsoon: Area and Intensity

[11] Figure 1 shows the observed and simulated global monsoon domains for the present climate. The multimodel ensemble mean of 29 CMIP5 models generally reproduces the observed global monsoon domain, although it tends to overestimate the areal extent in the NH and underestimate it in the SH, except in the African monsoon region (overestimate) and in North American monsoon region (underestimate). Models also have some difficulty in reproducing monsoon rainfall in East Asia. This underestimation of monsoon domain in East Asia was pointed out by *Kim et al*. [2008] for the CMIP3 models, and is not improved much in CMIP5 models.

[12] Changes in the global monsoon domain at the end of the 21st century under RCP8.5 scenario are also demarcated in Figure 1 with yellow and dark blue shadings, where yellow shading denotes shrinkage and dark blue shading denotes expansion of the monsoon domain, respectively. The CMIP5 model projections show that global monsoon area (GMA) expanding mainly over the central to eastern tropical Pacific, the southern Indian Ocean, and eastern Asia. A small area that extends from northeastern South America toward the ocean and another in the central tropical North Atlantic could represent also an expansion of the South American monsoon system and the tropical African monsoon, although the models overestimate monsoon area in northeastern South America. It is notable that the southwestern Japan and some part of the Korean peninsula, where the historical experiments underestimate precipitation amount, become monsoon domains due to increased precipitation in the RCP8.5 scenario.

[13] Figure 2 shows the scatter diagram of GMA and the global monsoon precipitation intensity (GMI) of two observed data sets (GPCP and CMAP) and each of 29 models for the present climate. Here GMI is the global monsoon precipitation amount per unit area [*Hsu et al*., 2011]. The observations themselves have about 10% uncertainty in estimating the GMA, with CMAP being larger than GPCP. Differences in aspects of the global monsoon assessed using GPCP and CMAP are discussed in *Hsu et al*. [2011]. Models have large variability both in reproducing GMA and GMI, but the multimodel ensemble closely matches the observations although with a slight overestimation. The future projections indicate larger values of GMA and GMI compared to present values. This feature is summarized in Figure 3, where GMA, GMI, and the global monsoon total precipitation (GMP) show an increase in the RCP4.5 scenario and more so in the RCP8.5 scenario at the end of the 21st century. This feature is consistent with other analyses using CMIP5 models [*Lee and Wang*, 2012; *Hsu et al*., 2012, 2013], and also similar to the findings using earlier CMIP3 models [*Hsu et al*., 2012, 2013]. The rates of change of GMA by the end of the 21st century compared with the present are –0.7, +5.4, and +9.4% (+0.4, +9.4, and +17.4%) for RCP4.5 (RCP8.5) at the 10th, 50th, and 90th percentiles, respectively. Almost all models show an increase, and only 3 out of 29 models show a decrease of GMA for RCP4.5, and two models for RCP8.5. Those two models are FGOALS-g2 and MIROC5 (as pointed out by *Hsu et al*. [2013]), where both models project a large precipitation decrease over the South Pacific Convergence Zone and over the Philippines Sea. This may be related to a projected strong La Niña-like SST anomaly in FGOALS-g2 and a large north-south hemispheric warming contrast in surface temperature in MIROC5. Both models failed to generate the western Pacific monsoon in their historical simulations [*Hsu et al*., 2013].

[14] Figure 3 shows that the rates of change of GMI are –0.5, +3.6, and +4.9% (–0.2, +5.5, and +8.5%) and those for GMP are –0.3, +9.0, and +12.6% (+4.9, +16.6, and +26.7%) for RCP4.5 (RCP8.5) at the 10th, 50th, and 90th percentiles, respectively. Based on the above multimodel results we conclude that monsoon-related precipitation is likely to significantly increase in a warmer climate.

[15] It is known that there is a linear relationship between global temperature change and global precipitation change among different models under one scenario and also among different scenarios [*Allen and Ingram*, 2002]. However, this

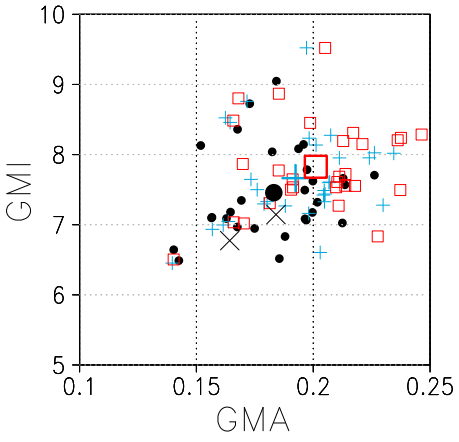

Figure 2. Scatter diagram between global monsoon area (GMA) and global monsoon intensity (GMI; mm d^{-1}) for observations and simulations. GPCP and CMAP values are shown as crosses. The present-day (future) simulations are displayed as closed circles, with plus signs for RCP4.5 future values and squares for RCP8.5). The large closed circle, large plus sign and large square denote the 29 CMIP5 multimodel means. GMA is scaled by global surface area.

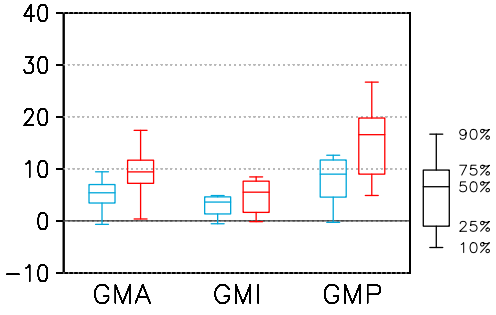

Figure 3. Future change (%) in GMA, GMI, and global monsoon total precipitation (GMP). Box-whisker plots in blue (red) are for the RCP4.5 (RCP8.5) scenario. The 10th, 25th, 50th, 75th, and 90th percentiles refer to 3rd, 8th, 15th, 22nd, and 27th values in ascending order among the 29 CMIP5 models, respectively.

is not the case for monsoon precipitation changes. *Hsu et al*. 2013 found no significant linkage between the increase in global mean surface temperature and the GMP/GMI change rates in CMIP5 models with the RCP4.5 scenario. The ratio of surface air temperature change between the present (1986–2005) and future (2080–2099) in RCP8.5 to that in RCP4.5 is about 2.0. However, the ratio in GMI is far less than this value. No linkage between the temperature change and the monsoon precipitation change is found in any regional monsoon domain except for South Asia, where a positive correlation is found (not shown).

[16] Time series of summer precipitation anomalies over the land global monsoon domain are displayed in Figure 4a. Figures 4b and 4c show those for the NH land and SH land, while Figure 4d is for the ocean-only parts of the global monsoon domain. Previous results showed that the observed global monsoon precipitation over land experienced a slight increasing trend from 1900 through the early 1940s, then an overall decreasing trend from the 1940s to the 1980s, followed by a recovering trend until the present [e.g., *Zhang and Zhou*, 2011; *Hsu et al*., 2011]. The different observed data sets shown in Figure 4a support these findings. CMIP5 models are not able to reproduce the mid-20th century maximum, but reproduce a gradual decline from the early 20th century until the 1980s, and project an increase throughout the 21st century. The recent trend of global land summer monsoon precipitation during 1985–2004 is +0.157 mm d^{-1} per 20 years in GPCP and +0.263 mm d^{-1} per 20 years in CMAP. The 29 CMIP5 models' mean trend is +0.090 mm d^{-1} per 20 years, which is about a half of the observations, but the positive trend simulated by models is consistent in sign with the observed trend during this period. However, regional-scale model-data comparisons of precipitation trends are difficult because of various problems including model skill, nature variability, and uncertainty in the observations, although there have been some attempts to detect and attribute zonal mean precipitation trends [*Zhang et al*., 2007] and precipitation extremes at the hemispheric scale [*Min et al*., 2011].

[17] The CMIP5 multimodel mean shows a larger increase of precipitation over the global land monsoon domain in the RCP8.5 scenario than in the RCP4.5 scenario. As indicated by the 10th and 90th percentile lines, model spread is quite large (and larger in RCP8.5 than in RCP4.5). As shown in Figures 4b and 4c, there is a clear contrast between NH and SH. The decreasing trend observed in the land global monsoon from the 1940s to the 1980s (Figure 4a) is evident in the NH land monsoon domain. Future projected increases are larger in NH than in SH as pointed out by *Lee and Wang* [2012]. The spread is larger over SH land than over NH

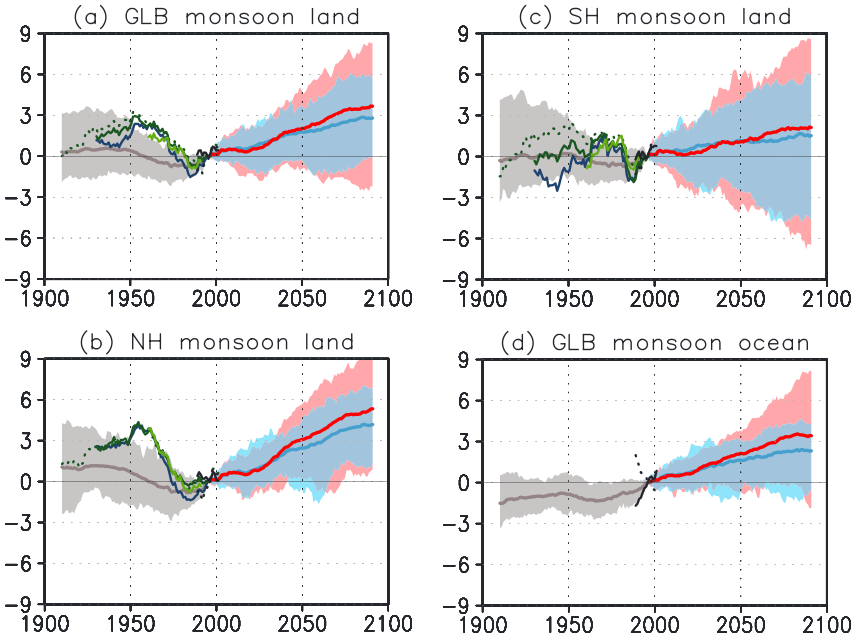

Figure 4. Time series of observed and simulated summer precipitation anomalies (%; 20 year running means) relative to the base period average (1986–2005, except GPCC VASClimO (1986–2000)) for the land monsoon domain over (a) globe, (b) Northern Hemisphere, (c) Southern Hemisphere, and for (d) the ocean global monsoon domain. The monsoon domains defined for the base period are fixed for the whole period. For the time series of simulations, Historical (grey), RCP4.5 (blue), and RCP8.5 (red) simulations by 29 CMIP5 model ensembles are shown in the 10th and 90th percentile (shading), and in all model averages (thick lines). For the time series of observations, Climatic Research Unit Time-Series 3.1 (dark blue), and GPCC v.6 (deep green with solid line) are calculated using only grid boxes (2.5 degree in lon./lat.) where at least one observation site exists for more than 80% of the target period (1921–2005). GPCC VASClimO (light green), GPCC v.6 (deep green with dots), GPCP (black), and CMAP (black with dots) are calculated using all grids for the period (1901–2010 for GPCC v.6; 1951–2000 for GPCC VASClimO; 1979–2010 for GPCP and CMAP).

land. Over NH land, more than 90% of models project an increase of monsoon precipitation in the late 21st century for both scenarios. Over the ocean monsoon domain, models simulate an increasing trend both in the 20th and 21st centuries (Figure 4d). The differences in the rainfall trends between RCP4.5 and RCP8.5 results are not statistically significant, despite remarkable temperature differences between the two scenarios, probably due to large variability among the models.

4. Regional Aspects of Future Monsoon Precipitation Changes

4.1. Validation of Regional Monsoons

[18] Despite an overall projected trend toward increasing global monsoon precipitation, the regional monsoons may have different responses in terms of precipitation and circulation features because the mechanisms at work may be different [*Cherchi et al.*, 2011]. Here we define seven monsoon regions: North America (NAM), South America (SAM), North Africa (NAF), South Africa (SAF), East Asia (EAS), South Asia (SAS), and Australia (AUS) (see Figure 5a for each domain). Figure 5 compares the present-day climate of CMIP5 models against two observational data sets for averaged precipitation (Pav), simple precipitation daily intensity index (SDII), seasonal maximum 5 day precipitation total (R5d), seasonal maximum consecutive dry days (CDD), monsoon onset date (ONS), retreat date (RET), and duration (DUR) over each regional land monsoon domain. The cross and rectangle denote TRMM3B42 and GPCP 1DD, respectively, calculated from 2.0 × 2.0 degree regridded data during the period 1998–2010. The extreme precipitation indices for

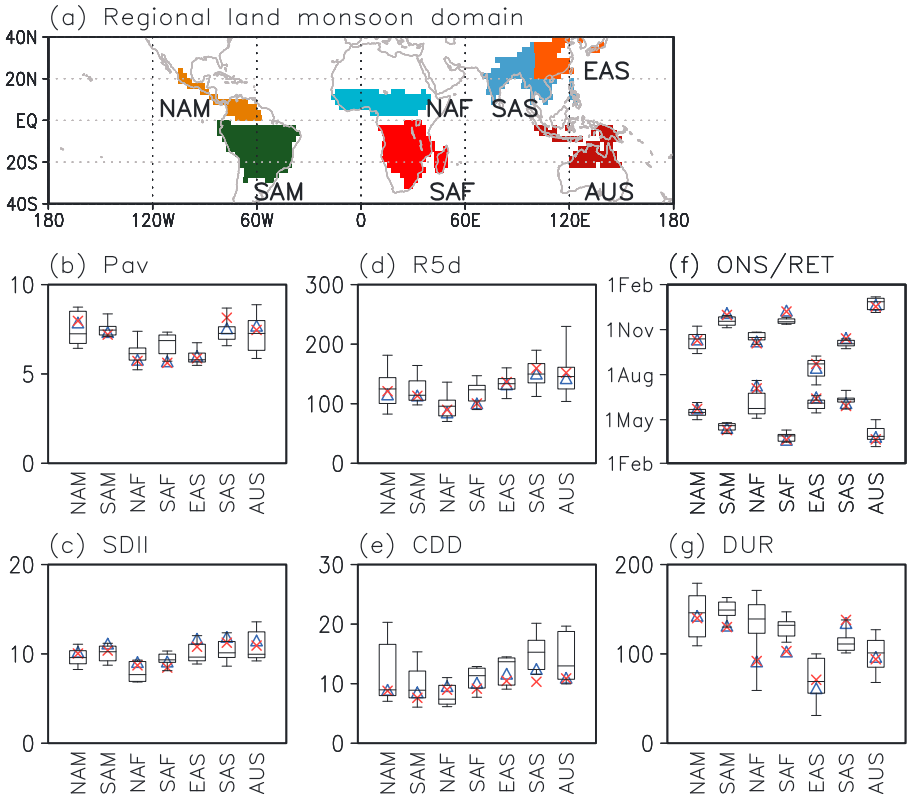

Figure 5. Validation of CMIP5 models against two observational data sets for (b) averaged precipitation (Pav), (c) simple precipitation daily intensity index (SDII), (d) seasonal maximum 5 day precipitation total (R5d), (e) seasonal maximum consecutive dry days (CDD), (f) monsoon onset date (ONS) and retreat date (RET), and (g) duration (DUR) over each regional land monsoon domain, based on daily data with original horizontal resolution from 21 CMIP5 models. Units are mm day^{-1} in Figures 5b and 5c, mm in Figure 5c, and days in Figures 5e–5g. The crosses and triangles denote TRMM3B42 and GPCP1DD, respectively, calculated from 2.0 × 2.0 degree regridded data during the period 1998–2010. Box-whisker plots are for the historical simulation (1986–2005). The 10th, 25th, 50th, 75th, and 90th percentiles refer to the 3rd, 6th, 11th, 16th, and 19th values in ascending order among the 21 models, respectively. All these indices are calculated over land monsoon domains determined by each model for the summer season (NH: MJJAS, SH: NDJFM) for the present-day. As an example, the regional land monsoon domain based on 21 multimodel mean precipitation in the present-day is shown in Figure 5a. For regional divisions, the equator separates the northern monsoon domains (EAS, NAM, NAF, and SAS) from the southern monsoon domains (SAM, SAF, and AUS), 60°E separates NAF from SAS, and 20°N and 100°E separates SAS from EAS. All the regional domains are within 40°S to 40°N.

the models are at first calculated on their original grid and then averaged over the regional monsoon domains determined by each model.

[19] It is revealed that the CMIP5 models in their present-day climate simulations reproduce the observations reasonably well in various aspects of regional monsoon precipitation, although scatter among models is large and with some outliers. For SAF, models systematically overestimate Pav, SDII, and R5d. For EAS, models underestimate Pav. These biases lead to overestimation or underestimation of regional monsoon area in these regions, depending on the sign of bias (Figure 1). Models tend to overestimate CDD except for NAF where models underestimate CDD. In other regions, more than half of the models are close to the observations of precipitation and its extremes.

[20] Monsoon seasonality (ONS, RET, and DUR) is more difficult to simulate. Only for NAM and AUS do models reasonably well simulate ONS, RET, and DUR. For SAM, simulated monsoon duration is longer than the observed due to earlier onset and slightly later retreat. For NAF, scatter among models is very large with earlier onset, later retreat and longer duration. For SAF, earlier onset results in longer duration. For EAS, models show earlier onset, while for SAS, later onset and earlier retreat result in shorter monsoon duration. Therefore, based on analysis of the above regions and variables, caution may be needed for interpretation of the future projections presented below.

4.2. Change Ratio of Pav, SDII, R5d, and DD for Seven Monsoon Regions Over Land

[21] Figure 6 shows geographical distributions of future change ratios (%) in Pav, SDII, R5d, and CDD during local summer season (MJJAS in NH; NDJFM in SH), based on 21 CMIP5 models. As with CMIP3 model results [*Meehl and coauthors*, 2007], CMIP5 models show Pav increases in the tropics and Pav decreases in the subtropics. Spatial patterns of SDII and R5d generally agree with those of Pav, but over some areas, where Pav decreases such as over the Mediterranean region and Central America, precipitation intensity is projected to increase. CDD is projected to increase over most tropical and subtropical regions except for the equatorial Pacific.

[22] Figure 7 shows change ratios (%) in Pav, SDII, R5d, and CDD during local summer season over each of the regional land monsoon domains, as determined by each model in the present-day climate. Table 2 shows the model

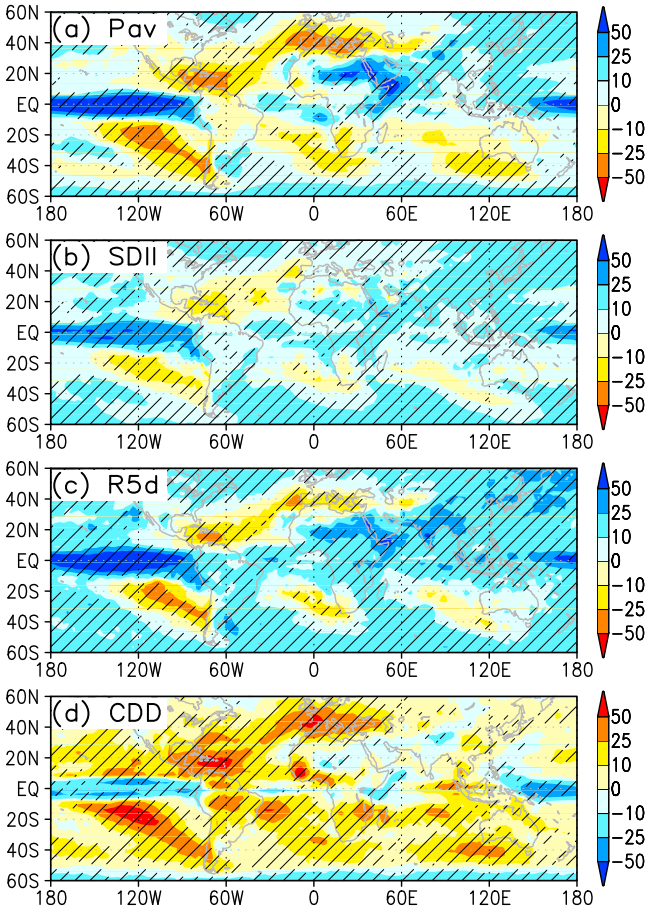

Figure 6. Future change ratio (%) for (a) averaged precipitation (Pav), (b) simple precipitation daily intensity index (SDII), (c) seasonal maximum 5 day precipitation total (R5d), and (d) seasonal maximum consecutive dry days (CDD) for the summer season (MJJAS in NH; NDJFM in SH), based on 21 CMIP5 model projections under the RCP8.5 scenario. Hatching denotes areas where the changes are statistically significant at the 5% level.

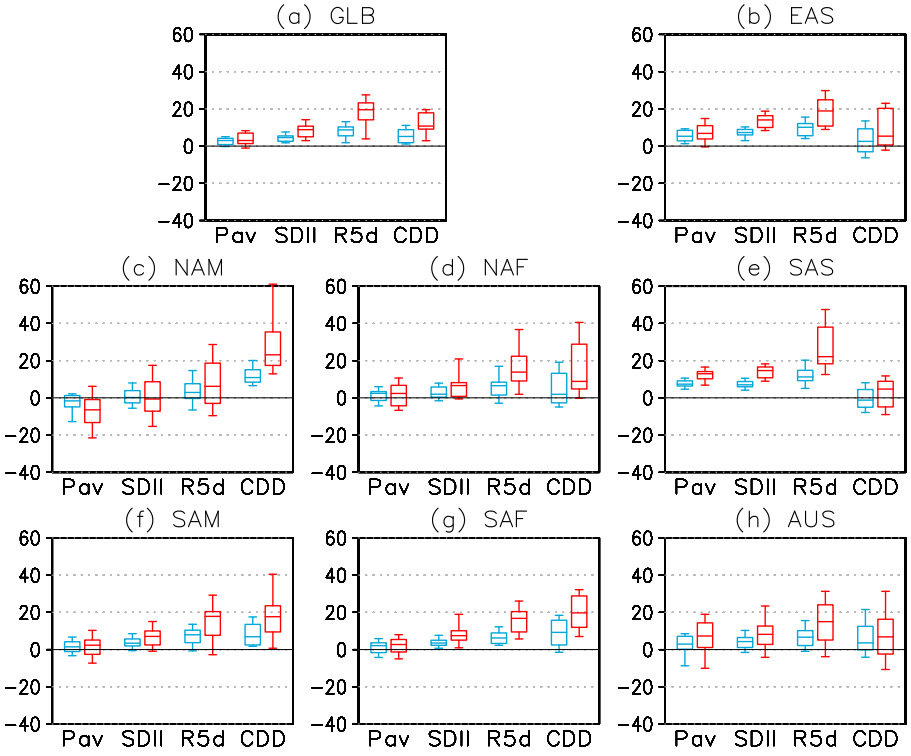

Figure 7. As in Figure 5, except for future change ratio (%) for averaged precipitation (Pav), simple precipitation daily intensity index (SDII), seasonal maximum 5 day precipitation total (R5d), and seasonal maximum consecutive dry days (CDD) over (a) global land monsoon domain, and (b)-(h) each regional land monsoon domain, based on daily data from 21 CMIP5 models. Box-whisker plots in blue (red) are for the RCP4.5 (RCP8.5) scenario.

Table 2. Median (50th Percentile) Values of Precipitation Indices in Median (50th Percentile) Over Each Regional Land Monsoon Domain. (a) Present-Day Climate Simulation. (b) Future Change. (c) Future Percentage Change (%)

(a) Present-day climate

	Pav	SDII	R5d	CDD
NAM	7.2	9.6	124.8	9.0
SAM	7.5	10.2	114.3	8.9
NAF	6.1	7.7	95.8	7.4
SAF	6.9	9.3	123.4	11.3
EAS	5.8	9.6	133.7	13.7
SAS	7.3	10.1	149.8	15.3
AUS	7.3	10.0	145.6	13.0

(b) Future change

	Pav		SDII		R5d		CDD	
	RCP4.5	RCP8.5	RCP4.5	RCP8.5	RCP4.5	RCP8.5	RCP4.5	RCP8.5
NAM	–0.12	–0.46	0.01	–0.06	3.8	9.6	0.99	2.40
SAM	0.11	0.19	0.32	0.69	9.5	21.0	0.72	1.50
NAF	0.17	0.13	0.17	0.47	5.4	14.6	0.13	0.76
SAF	0.12	0.15	0.32	0.67	7.6	21.1	1.05	2.19
EAS	0.31	0.44	0.71	1.30	14.5	24.8	0.28	0.71
SAS	0.55	0.91	0.71	1.48	18.7	33.7	-0.21	0.80
AUS	0.19	0.53	0.44	0.85	11.7	23.6	0.42	0.68

(c) Future percentage change

	Pav		SDII		R5d		CDD	
	RCP4.5	RCP8.5	RCP4.5	RCP8.5	RCP4.5	RCP8.5	RCP4.5	RCP8.5
NAM	–1.6	–6.5	0.2	–0.7	2.9	6.2	10.9	23.1
SAM	1.5	2.4	3.4	7.1	7.9	17.8	6.9	17.7
NAF	2.4	2.4	1.9	6.6	6.6	13.8	1.9	8.8
SAF	2.1	2.7	3.5	7.5	6.2	16.8	9.2	19.7
EAS	5.3	6.8	7.3	14.1	10.1	18.9	2.5	5.4
SAS	7.3	12.9	7.0	14.7	11.2	22.1	–1.2	4.7
AUS	2.9	7.3	4.3	8.2	6.7	15.0	3.6	6.8

median (50th percentile) values of precipitation indices, in terms of mm d^{-1} or days, over each regional land monsoon domain for the present-day climate, and for future changes.

[23] In the NAM region, Pav is projected to decrease, more so in RCP8.5 than in RCP4.5. The average projected SDII change is around zero with the models evenly divided on positive or negative changes, but R5d is projected to increase in more than two thirds of models. In the SAM region, although the median Pav change is small, two thirds of models indicate an increase of precipitation in this region. In SAM, most models project an increase in the precipitation extreme indices (SDII and R5d) in both RCP4.5 and RCP8.5 scenarios, with larger change ratios in the latter. The number of consecutive dry days is projected to increase both in NAM and SAM.

[24] In Africa, changes in Pav are insignificant both in the NAF region and in the SAF region in both scenarios. SDII and R5d are projected to increase in both scenarios for both African monsoon regions. Model agreement is higher in the RCP8.5 scenario in NAF. This is also the case with the increase in consecutive number of dry days in the future.

[25] Over the Asian monsoon domain, the median increase rate for precipitation is larger than that over other monsoon domains, indicating that the sensitivity of Asian monsoon to global warming is stronger than that of other monsoons. Over the EAS region, more than 85% of models show an increase in Pav, while more than 95% of models project an increase in SDII and R5d. Also, many models project an increase in CDD. Future increases in precipitation extremes in the SAS region are projected by all models in both scenarios. However, agreement among models in projecting changes in CDD is low. Given the large population residing in these two regions, the variability of extreme events needs to be studied more comprehensively.

[26] Over the AUS region, many models agree in projecting an increase of Pav and SDII in both scenarios, while agreement is better for R5d increase. CDD is also projected to increase in the future but model scatter becomes large in RCP8.5.

[27] There are differences in the projections in NAM depending on whether the regional monsoon domains are fixed at the present-day domains (Figure 7c), or determined separately for the present-day and for the future. In the latter case, the percentage changes in median values under RCP8.5 are –0.3%, +5.6%, and +13.4% for Pav, SDII, and R5d, respectively, indicating more intense heavy precipitation.

[28] In summary, heavy precipitation indices are projected to increase much more than the mean precipitation over all regional monsoon domains. As the atmosphere becomes more stable, the frequency of precipitating events decreases (CDD increases), but the precipitation intensity can be stronger once an event occurs because more moisture is available in a warmer atmosphere. It is also found that the change rates for SDII, R5d, and CDD depend more on the emission scenario compared to those for mean precipitation. Over the Asian monsoon regions, projected changes in extreme precipitation indices of Pav, SDII, and R5d are larger than those in the other monsoon regions. On the other hand, over the American and

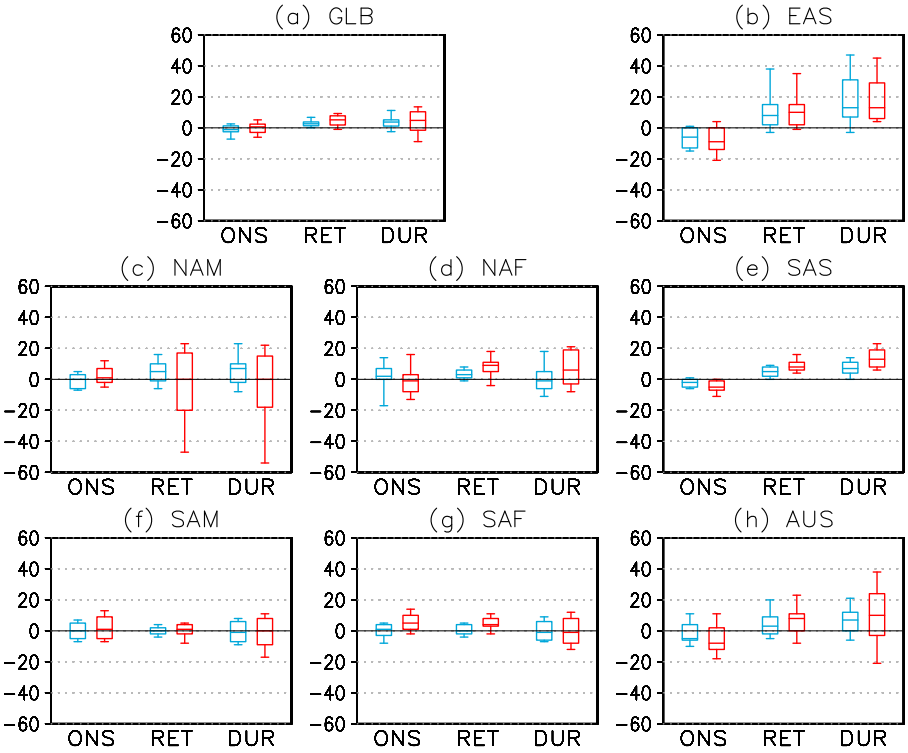

Figure 8. As in Figure 7, except for future changes (days) in monsoon onset date (ONS), retreat date (RET) and duration (DUR) over each regional land monsoon domain. For calculation of the global monsoon domain statistics in Figure 8a, the seven regional monsoon domain statistics were averaged with weighting based on their area in the present-day.

African monsoon regions, expected future changes in Pav are rather modest, but those in R5d are large and comparable to those noted over the Asian monsoon regions.

4.3. Change of Monsoon Seasonality

[29] Timings of monsoon onset, retreat, and thus the monsoon duration are also expected to change in the future. Many indices have been proposed to define monsoon onset and retreat [e.g., *Zeng and Lu*, 2004; *Wang et al.*, 2004; *Silva and Carvalho*, 2007; *Kajikawa et al.*, 2010]. In this study, we follow the method proposed by *Wang and LinHo* [2002] based on precipitation exceeding (or dropping below) a threshold value (see section 2.3). Figure 8 shows projected future changes in monsoon onset date, retreat date, and duration over each of the regional land monsoon domains. Here positive numbers for onset and retreat indicate a delay. The CMIP5 models project that monsoon retreat dates will delay, while onset dates will either advance or show no

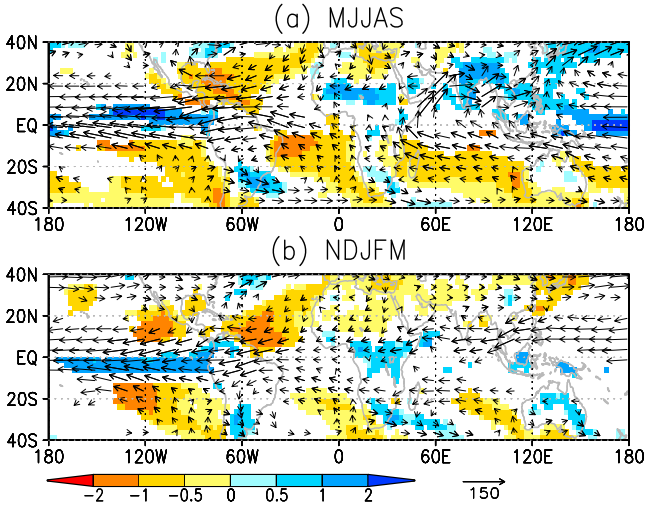

Figure 9. Changes in vertically integrated water vapor flux (vector; kg m^{-1} s^{-1}) and its convergence (shading; mm d^{-1}) between the present-day (1986–2005) and the future (2080–2099) in the RCP8.5 scenario for (a) MJJAS and (b) NDJFM, based on the 23 CMIP5 multimodel mean. Only changes that have the same sign in more than 80% of models (i.e., 19 models) are shown.

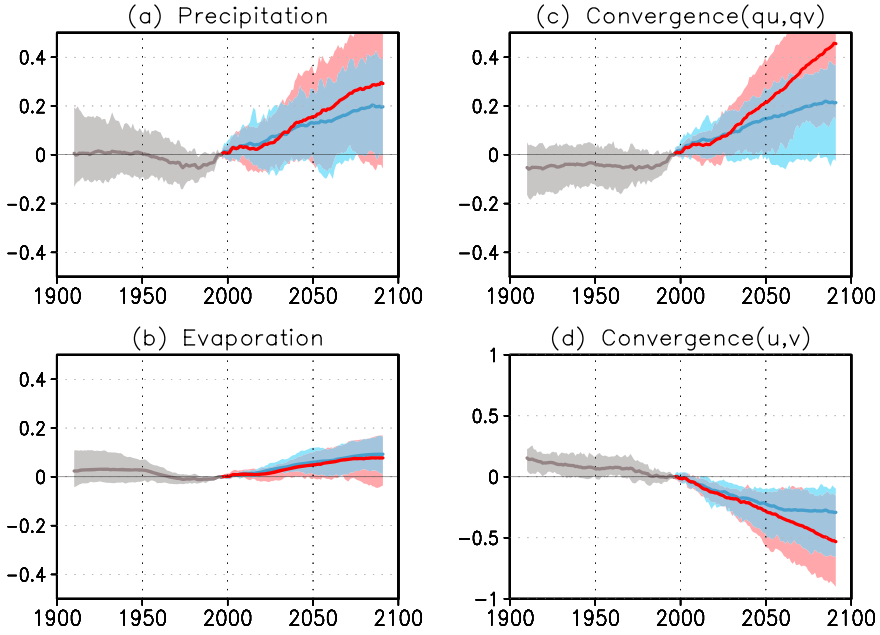

Figure 10. Time series of simulated anomalies over global land monsoon domain for (a) precipitation (mm d^{-1}), (b) evaporation (mm d^{-1}), (c) water vapor flux convergence in the lower (below 500 hPa) troposphere (mm d^{-1}) and (d) wind convergence in the lower troposphere (10^{-3} kg m^{-2} s^{-1}), relative to the base period average (1986–2005), based on 23 CMIP5 model monthly outputs. Historical (grey), RCP4.5 (blue), and RCP8.5 (red) simulations are shown in the 10th and 90th percentile (shading), and in all model averages (thick lines).

change, resulting in lengthening of the monsoon season in many regions. In particular, such features are very conspicuous in SAS, where model agreement is high with earlier onset, later retreat and longer duration. More than 85% (95%) of models project later retreat in SAS in RCP4.5 (RCP8.5). The same is found with the CMIP3 models [*Kumar and coauthors*, 2011]. This is also consistent with recent observation of advanced South Asian monsoon onset in recent decades [*Kajikawa et al*., 2012]. In AUS, earlier onset, later retreat, and longer duration are projected. In EAS, many models also project earlier onset and longer duration, but the spread among models is very large. *Kitoh and Uchiyama* [2006] investigated the changes in monsoon seasonality of 15 CMIP3 models, and found late retreat over the region extending from Taiwan, Ryukyu Islands to the south of Japan. In their study, however, significant changes were found over the East Asian oceanic monsoon region, where recent CMIP5 models' performance is very poor in reproducing monsoon rainfall (Figure 1).

[30] In contrast to other regions, slightly later onset is projected in NAF in RCP4.5, where many models show later retreat. Monsoon duration is not projected to change (RCP4.5) or becomes longer (RCP8.5). In SAF, only in RCP8.5, later onset and later retreat (no change in duration) are projected. There is low agreement among models in the change of onset, retreat and duration in NAM and SAM.

[31] As implied by the large spread among models in most regions, projection of changes in monsoon seasonality may be sensitive to the way the monsoon onset and retreat are defined. However, we find that monsoon onset dates are generally projected to come earlier or not change much, and monsoon retreat dates are projected to be delayed, resulting in a general lengthening of the monsoon season.

5. Discussions and Summary

[32] Future projections indicate an overall increase of monsoon precipitation over land that is primarily explained by anomalous water vapor flux convergence into these regions (Figure 9). However, this is not a direct consequence of tropical circulation changes. Model experiments project surface as well as air temperature increases in the 21st century. At the surface, warming is greatest over land and at high northern latitudes [*Meehl and coauthors*, 2007]. This leads to greater land-sea surface temperature contrast with lower surface pressures over land and higher surface pressures over ocean in summer. Due to a rise in air temperature, water vapor in the atmosphere increases nonlinearly with temperature. This increase in precipitable water is, to first order, responsible for the increase in precipitation, particularly in middle to high latitudes. In the global monsoon region, the situation is more complex, where changes in the atmospheric circulation also matter and land-ocean contrast is a key mechanism [*Fasullo*, 2012]. The tropical atmosphere responds in such a way that the strength of the atmospheric overturning circulation decreases as the climate warms [*Vecchi and Soden*, 2007]. The explanation is based on thermodynamic arguments [*Allen and Ingram*, 2002; *Held and Soden*, 2006] and is also related to a reduction of radiative cooling in the lower troposphere due to CO_2 increase where the overlap effect of the CO_2 and water vapor absorption bands play a crucial role [*Sugi and Yoshimura*, 2004]. Figure 10 shows the time-series of precipitation, evaporation, lower-troposphere water vapor flux convergence, and lower-troposphere wind convergence averaged over the global monsoon domain over land. From Figure 10d, it is clear that the CMIP5 models show a decreasing trend of lower-troposphere wind convergence (dynamical factor) throughout the 20th and 21st centuries. When moisture build-up effect is considered, moisture flux convergence shows a different story (thermodynamic factor, Figure 10c). In the 20th century, moisture convergence over the global land monsoon domain is almost constant until around 1980, and then turns into an increasing trend in the 21st century. This implies that the moisture increase due to temperature rise overwhelms the weakening of the large-scale circulation, thus resulting in increased moisture flux and its convergence around 1980, which is responsible for the intensification of mean monsoon rainfall, leading to the "wet-get-wetter" [*Held and Soden*, 2006] or "warmer-get-wetter" [*Xie and Coauthors*, 2011] paradigms. Surface evaporation showed a decreasing trend from the mid-20th century probably due to aerosol increase [*Turner and Annamalai*, 2012], but it also turned to an increase around the 1980s due to warmer surface temperatures (Figure 10b). Therefore, the increase of the global monsoon precipitation in the future can be attributed to the increase of moisture convergence due to increased water vapor in the air column and surface evaporation, offset to a certain extent by the weakening of the monsoon circulation.

[33] Contributions from other factors are plausible for the changes in each regional monsoon. The weakening circulation over the Indian monsoon region [*Ramesh and Goswami*, 2007] is perhaps a regional phenomenon, brought about by changes in local gradients and convergence. Existence of the Tibetan high is associated with an establishment of a large-scale thermal contrast between the Asian land mass and neighboring oceans [*Li and Yanai*, 1996; *Wu et al*., 2012]. However, in the air above, models consistently project enhanced upper-tropospheric warming in the tropics [*Meehl and coauthor*s, 2007]. This is related to increasing condensational heating in the future climate. The upper-troposphere over the Indian Ocean warms more than over the Tibetan plateau, reducing the meridional thermal gradient between the Asian continent and adjacent oceans, thus leading to a weakening of the Asian summer monsoon circulation [*Ueda et al*., 2006].

[34] Changes in global monsoon precipitation were also investigated by *Hsu et al*. [2012, 2013] and *Lee and Wang* [2012]. *Hsu et al*. [2012] used 24 CMIP3 models under the SRES A1B scenario and 11 CMIP5 models under the RCP4.5 scenario, *Hsu et al*. [2013] used 19 CMIP5 models under the RCP4.5 scenario, while *Lee and Wang* [2012] used four selected models from 20 CMIP5 models under the RCP4.5 scenario along with the same four CMIP3 models under the SRES A1B scenario. They all reached the conclusion that global monsoon precipitation is likely to increase in the 21st century. *Lee and Wang* [2012] also noted a greater northern-southern hemispheric asymmetry and eastern-western hemispheric asymmetry in the future. Our conclusion based on 29 CMIP5 models is consistent with the above findings. Our comparison between RCP4.5 and RCP8.5 scenarios indicates larger and more robust changes in global monsoons in a warmer RCP8.5 world.

[35] To sum up, the state-of-the-art climate models project that the global monsoon precipitation is likely to strengthen in the 21st century with increase in its area as well as its intensity, while monsoon circulation weakens. Overall climate change projections obtained with CMIP5 models are similar to those from CMIP3 models. Considering the improvements in CMIP5 models against CMIP3 models [*Sperber et al.*, 2012], we have now more confidence in the results. Changes in climate phenomena such as El Niño-Southern Oscillation can modulate regional monsoons. However, assessing possible roles of changes in such climate phenomena for each monsoon system is beyond the scope of this study. Currently, atmospheric aerosol loading is influencing regional climate in various ways, such as a black carbon-induced enhancement and a sulfate-induced suppression of regional monsoon precipitation [*Turner and Annamalai*, 2012]. Most CMIP5 models adopted in this study include both the direct and indirect effect of aerosols. As we advance into the 21st century, the relative effect of aerosols may be overwhelmed by the effect of increasing greenhouse gases, but we do not yet know the exact consequences in a quantitative way. This is one of the uncertainties in precisely assessing the future state of the monsoon.

[36] **Acknowledgments.** We acknowledge the World Climate Research Programme's Working Group on Coupled Modelling, which is responsible for CMIP, and we thank the climate modeling groups for producing and making available their model output. For CMIP the U.S. Department of Energy's Program for Climate Model Diagnosis and Intercomparison provides coordinating support and led development of software infrastructure in partnership with the Global Organization for Earth System Science Portals. Work by H.E. was partially supported by the Environment Research and Technology Development Fund (A-1201) of the Ministry of the Environment, Japan. A.K. and H.E. thank Osamu Arakawa for the data management. I.F.A.C. thanks CNPq for research support.

References

Allen, M. R., and W. J. Ingram (2002), Constraints on future changes in climate and the hydrologic cycle, *Nature*, *419*, 224–232.

Beck, C., J. Grieser, and B. A. Rudolf (2005), New Monthly Precipitation Climatology for the Global Land Areas for the Period 1951 to 2000, *DWD Klimastatusbericht*, *2004*, 181–190.

Cherchi, A., A. Alessandri, S. Masina, and A. Navarra (2011), Effects of increased CO2 levels on monsoons, *Clim. Dyn.*, *37*, 83–101.

Fasullo, J. (2012), A mechanism for land-ocean contrasts in global monsoon trends in a warming climate, *Clim. Dyn.*, *39*, 1137–1147.

Held, I. M., and B. J. Soden (2006), Robust responses of the hydrological cycle to global warming, *J. Climate*, *19*, 5686–5699.

Hsu, P.-C., T. Li, J.-J. Luo, H. Murakami, A. Kitoh, and M. Zhao (2012), Increase of global monsoon area and precipitation under global warming: A robust signal? *Geophys. Res. Lett.*, *39*, L06701.

Hsu, P.-C., T. Li, H. Murakami, and A. Kitoh (2013), Future change of the global monsoon revealed from 19 CMIP5 models, *J. Geophys. Res. 118*, doi:10.1002/jgrd.50145.

Hsu, P.-C., T. Li, and B. Wang (2011), Trends in global monsoon area and precipitation in the past 30 years, *Geophys. Res. Lett.*, *38*, L08701.

Huffman, G. J., R. F. Adler, D. T. Bolvin, and G. Gu (2009), Improving the global precipitation record: GPCP Version 2.1, *Geophys. Res. Lett.*, *36*, L17808.

Huffman, G. J., R. F. Adler, M. M. Morrissey, D. T. Bolvin, S. Curtis, R. Joyce, B. McGavock, and J. Susskind (2001), Global precipitation at one-degree daily resolution from multisatellite observations, *J. Hydrometeorol.*, *2*, 36–50.

Huffman, G. J., D. T. Bolvin, E. J. Nelkin, D. B. Wolff, R. F. Adler, G. Gu, Y. Hong, K. P. Bowman, and E. F. Stocker (2007), The TRMM multisatellite precipitation analysis (TMPA): quasi-global, multiyear, combined-sensor precipitation estimates at fine scales, *J. Hydrometeorol.*, *8*, 38–55.

Kajikawa, Y., B. Wang, and J. Yang (2010), A multi-time scale Australian monsoon index, *Int. J. Climatol.*, *30*, 1114–1120.

Kajikawa, Y., T. Yasunari, S. Yoshida, and H. Fujinami (2012), Advanced Asian summer monsoon onset in recent decades, *Geophys. Res. Lett.*, *39*, L03803.

Kim, H.-J., B. Wang, and Q. Ding (2008), The global monsoon variability simulated by CMIP3 coupled climate models, *J. Climate*, *21*, 5271–5294.

Kitoh, A., and T. Uchiyama (2006), Changes in onset and withdrawal of the East Asian summer rainy season by multi-model global warming experiments, *J. Meteor. Soc. Japan*, *84*, 247–258.

Kumar, K. K., and Coauthors (2011), The once and future pulse of Indian monsoonal climate, *Clim. Dyn.*, *36*, 2159–2170.

Lee, J.-Y., and B. Wang (2012), Future change of global monsoon in the CMIP5, *Clim. Dyn.*, doi:10.1007/s00382-012-1564-0.

Li, C., and M. Yanai (1996), The onset and interannual variability of the Asian summer monsoon in relation to land-sea thermal contrast, *J. Climate*, *9*, 358–375.

Li, Y., N. C. Jourdain, A. S. Taschetto, C. C. Ummenhofer, K. Ashok and A. Sen Gupta (2012), Evaluation of monsoon seasonality and the tropospheric biennial oscillation transitions in the CMIP models, *Geophys. Res. Lett.*, *39*, L20713, doi:10.1029/2012GL053322.

Marengo, J., and Coauthors (2010), Recent developments on the South American Monsoon system, *Int. J. Climatol.*, *32*, 1–21.

Meehl, G. A., and coauthors (2007), Global Climate Projections. in *Climate Change 2007: The Physical Science Basis. Contribution of Working Group I to the Fourth Assessment Report of the Intergovernmental Panel on Climate Change* edited by S. Solomon, et al. 747–845, Cambridge University Press, Cambridge, UK.

Min, S.-K., X. Zhang, F. W. Zwiers and G. C. Hegerl (2011), Human contribution to more-intense precipitation extremes, *Nature*, *470*, 378–381.

Mitchell, T. D., and P. D. Jones (2005), An improved method of constructing a database of monthly climate observations and associated high-resolution grids, *Int. J. Climatol.*, *25*, 693–712.

Raia, A., and I. F. A. Cavalcanti (2008), The life cycle of the South American Monsoon System, *J. Climate*, *21*, 2667–6246.

Ramesh, K. V., and P. Goswami (2007), Reduction in temporal and spatial extent of the Indian summer monsoon, *Geophys. Res. Lett.*, *34*, L23704.

Rudolf, B., H. Hauschild, W. Rueth, and U. Schneider (1994), Terrestrial Precipitation Analysis: Operational Method and Required Density of Point Measurements. *NATO ASI I/26, Global Precipitation and Climate Change*, edited by M. Desbois & F. Desalmand Springer Verlag, Berlin, pp 173–186.

Silva, A. E., and L. M. V. Carvalho (2007) Large-scale index for South America Monsoon (LISAM), *Atmospheric Science Letters*, *8*, 51–57.

Sperber, K. R., H. Annamalai, I.-S. Kang, A. Kitoh, A. Moise, A. G. Turner, B. Wang and T. Zhou (2012) The Asian summer monsoon: An intercomparison of CMIP5 vs. CMIP3 simulations of the late 20th century, *Clim. Dyn.*, doi:10.1007/s00382-012-1607-6.

Sugi, M., and J. Yoshimura (2004), A mechanism of tropical precipitation change due to CO2 increase, *J. Climate*, *17*, 238–243.

Taylor, K. E., R. J. Stouffer, and G. A. Meehl (2012), An overview of CMIP5 and the experiment design, *Bull. Amer. Meteor. Soc.*, *93*, 485–498.

Trenberth, K. E., D. P. Stepaniak, and J. M. Caron (2000), The global monsoon as seen through the divergent atmospheric circulation, *J. Climate*, *13*, 3969–3993.

Turner, A. G., and A. Annamalai (2012), Climate change and the South Asian summer monsoon, *Nature Climate Change*, *2*, doi:10.1038/NCLIMATE1495.

Ueda, H., A. Iwai, K. Kuwano, and M. E. Hori (2006), Impact of anthropogenic forcing on the Asian summer monsoon as simulated by eight GCMs, *Geophys. Res. Lett.*, *33*, L06703.

Vecchi, G. A., and B. J. Soden (2007), Global warming and the weakening of the tropical circulation, *J. Climate*, *20*, 4316–4340.

Vera, C., and Coauthors (2006), Toward a unified view of the American Monsoon System, *J. Climate*, *19*, 4977–5000.

Wang, B., and Q. Ding (2006), Changes in global monsoon precipitation over the past 56 years, *Geophys. Res. Lett.*, *33*, L06711.

Wang, B., and Q. Ding (2008), Global monsoon: Dominant mode of annual variation in the tropics, *Dynamics of Atmospheres and Oceans*, *44*, 165–183.

Wang, B., and LinHo (2002), Rainy season of the Asian-Pacific summer monsoon, *J. Climate*, *15*, 386–398.

Wang, B., H.-J. Kim, K. Kikuchi, and A. Kitoh (2011), Diagnostic metrics for evaluation of annual and diurnal cycles, *Clim. Dyn.*, *37*, 941–955.

Wang, B., LinHo, Y. Zhang, and M.-M. Lu (2004), Definition of South China Sea monsoon onset and commencement of the East Asia summer monsoon, *Climate*, *17*, 699–710.

Wang, B., Y. Liu, H.-J. Kim, P. J. Webster, and S.-Y. Yim (2012), Recent change of the global monsoon precipitation (1979-2008), *Clim. Dyn.*, doi:10.1007/s00382-011-1266-z.

Webster, P. J., and Coauthors (1998), Monsoons: processes, predictability, and the prospects for prediction, *J. Geophys. Res.*, *103*, 14451–14510.

Wu, G., Y. Liu, B. He, Q. Bao, A. Duan, and F.-F. Jin (2012), Thermal controls on the Asian summer monsoon, *Sci. Rep.*, *2*, 404: doi:10.1038/srep00404.

Xie, P.-P., and P. A. Arkin (1997), Global precipitation: A 17-year monthly analysis based on gauge observations, satellite estimates and numerical model outputs, *Bull. Amer. Meteorol. Soc.*, *78*, 2539–2558.

Xie, S. P., and Coauthors (2011), Global warming pattern formation: sea surface temperature and rainfall, *J. Climate*, *23*, 966–986.

Zeng, X., and E. Lu (2004), Globally unified monsoon onset and retreat indexes, *J. Climate*, *17*, 2241–2248.

Zhang, L., and T. Zhou (2011), An assessment of monsoon precipitation changes during 1901-2001, *Clim. Dyn.*, *37*, 279–296.

Zhang, X., F. W. Zwiers, G. C. Hegerl, F. H. Almbert, N. P. Gillett, S. Solomon, P. A. Stott and T. Nozawa (2007), Detection of human influence on twentieth-century precipitation trends, *Nature*, *448*, 461–465.

Zhou, T., R. Yu, H. Li, and B. Wang (2008a) Ocean forcing to changes in global monsoon precipitation over recent half-century, *J. Climate*, *21*, 3833–3852.

Zhou, T., L. Zhang, and H. Li (2008b), Changes in global land monsoon area and total rainfall accumulation over the last half century, *Geophys. Res. Lett.*, *35*, L16707.